Patient-specific finite element analysis of popliteal stenting

Michele Conti[a,], Michele Marconi[b], Giulia Campanile[a], Alessandro Reali[a], Daniele Adami[b], Raffaella Berchiolli[b], Ferdinando Auricchio[a]

[a] *Dept. of Civil Engineering and Architecture (DICAr), University of Pavia, Pavia, Italy.*
[b] *Vascular Unit, IRCCS Cisanello, Pisa, Italy*
[c] *Institute for Advanced Study, Technische Universität München, Garching, Germany*

Abstract

Nitinol self-expanding stents are used to treat diseased peripheral vessels such as the popliteal artery. Unfortunately, the complex vessel kinematics characterising the knee flexion leads to severe loading conditions, often inducing the device failure. For this reason, it is essential to analyze the artery configuration change during the leg flexion and its impact on the mechanical solicitation of the implanted stent.
Given these considerations, in the present study we reconstruct the patient-specific popliteal kinematics from Computed Tomography Angiography through image analysis and segmentation; subsequently, we impose the reconstructed configuration change of the artery to a stent model virtually implanted in the artery through structural finite element analysis (FEA).
The results indicate that the vessel configuration changes significantly during the knee flexion, leading to a non-uniform increase of the vessel curvature especially above the knee. The resulting stent loading reflects such a non-uniform change as the stent portion located above the knee experiences a more severe solicitation when compared to its remaining part.
Despite limited to one specific case, the study highlights the importance of the non-uniform, complex, and three dimensional biomechanical solicitations for design of popliteal stents, underlining the potential key-role of dedicated patient-specific FEA simulations.

Keywords: finite element analysis (FEA), biomechanics, popliteal stenting, patient-specific, nitinol.

1. Introduction

The popliteal artery (PA) is located behind the knee; it is a direct extension of the superficial femoral artery (SFA), after passing through the adductor hiatus, an opening in the tendinous slip of the great adductor muscle of the thigh [1]. Although the popliteal artery is a relatively short vascular segment, it could suffer a unique set of pathologic conditions such as atherosclerotic stenosis [2] or aneurysm [3]. Popliteal arteries are indeed the most frequent location of aneurysms after the abdominal aorta aneurysms and, despite an incidence lower than 0.1%, it represents the majority of peripheral aneurysms [4]. The natural history of popliteal artery aneurysm is characterized by the onset of complications such as thrombosis and embolization that can lead to limb loss in about 20% of the cases [5]. Aneurysm endovascular treatment is based on sac exclusion by the covered stent but, at the moment, the stent does not ensure the same results of bypass, that is considered the gold standard [6] because, also in this case, there are concerns related to the device failure due the complex vessel kinematics [7].
Given such considerations, it is clear that a focused engineering effort is required to quantitatively assess: 1) the PA kinematics; 2) the mechanical response of stent-like devices implanted in this vascular region. Although various contributions about these two issues are already available in the literature, there is still

*Corresponding author: Michele Conti, Dept. of Civil Engineering and Architecture (DICAr), Pavia University, Via Ferrata 3, 27100, Pavia, Italy. Email address: michele.conti@unipv.it

a lack of integration between them especially from the perspective of the patient-specific analysis. For this reason, in the present study we reconstruct the PA kinematics from medical images imposing then the computed vessel displacement as a loading condition to a stent model in order to evaluate its solicitation in a realistic conditions. In particular, we have elaborated two Computed Tomography Angiography (CTA) datasets of the leg, one in straight position and one in bent position, to compute how the vessel shape changes during the leg bending. Subsequently, we have performed structural finite element analysis (FEA) of the stent deformation under the action of reconstructed vessel kinematics.

2. Materials and Methods

In this section we discuss the adopted workflow, which can be thought as the integration of two main stages: i) the medical image analysis; ii) the structural finite element analysis. The first stage is aimed at assessing how the popliteal artery deforms during the leg bending while the second stage is aimed at computing the stress/strain distribution along the stent structure when solicited by the vessel kinematics. Given such a workflow, in the following we first summarize the clinical case under investigation. Then we discuss the medical image elaboration concluding the section with the description of the FEA set-up.

2.1. Image processing: segmentation and reconstruction of artery kinematics

We analysed the case of a 66 years-old patients with an aneurysm of the right poplitea as shown in Figure 1. One of key steps of our study is the analysis of PA vascular anatomy when the leg is straight or bent. For this reason, we have performed an accurate image processing of two CTA datasets: i) scan performed with the leg in straight position; ii) scan performed with the leg in bent position. As highlighted by Figure 2, our input data is the 3D configuration of the right leg when it is in the straight position, i.e., the angle θ between the femur and the tibia is 180°, and when it is in the bent position, i.e., the angle θ is almost 220°. Thus, we are considering the case where the PA configuration change is due to a knee flexion of almost 40°. All data from the CTA examination were saved digitally on a data-storage workstation and anonymized prior to the medical image analysis.
For each CTA dataset, we perform an accurate image segmentation using the method called *snake evolution* implemented in the open-source software ITK-Snap [8], obtaining the 3D reconstructions of the PA lumen, leg bones, and vessel calcification for both configurations as depicted in Figure 3.
The resulting 3D models can be exported in stereolithography representation (STL format), which can be subsequently elaborated for our simulation purposes. Given the straight and bent 3D lumen profiles, we have performed a geometrical analysis of them to evaluate the change of vessel anatomy induced by knee flexion. The operations are described as follows. Firstly, we have registered the PA lumen profile in straight configuration onto the bent one using the module *vmtkicpregistration*, available within the library Vascular Model Toolkit (VMTK - www.vmtk.org), secondly we have computed the lumen centerline for both cases using the VMTK module *vmtkcenterlines* as depicted in Figure 3.
The goal of the centerline computation is two-folded: i) evaluation of the configuration change of the artery due to the knee flexion; ii) generation of the input for the setting of structural FEA as discussed in the following subsection. It is worth noting that we use the calcifications and the vessel bifurcations as *reference* anatomical points to define the beginning and the end of each centerline, in order to ensure a congruent comparison of them.

Figure 2

Figure 3

2.2. Simulation set-up

2.2.1. Reconstruction of the vessel kinematics

As described in the previous subsection, from the medical image analysis we have obtained two basic information: i) the PA centerline when the leg is in the straight position, and ii) the PA centerline when the leg is in the bent position. Consequently, these two data represent somehow the starting and final configuration of the artery during a knee flexion movement. Under the hypothesis that the path followed by each centerline point, during the leg bending, coincides with the straight line connecting its starting and final position, we can use the computed data to reconstruct the configuration change of the artery. Given such a consideration, we use the centerline path at the different time frames as sweeping path of a rigid tubular surface, here labeled as *vessel*, which drives the stent deformation during the FEA, implementing thus the approach depicted in Figure 4 and already discussed in our previous studies [9, 10, 11]. It is worth noting that such an approach can be justified by the working hypothesis that the vessel kinematics remains the same after stent implant, although we acknowledged that such an hypothesis is quite strong. The numerical analysis is non-linear, involving large deformations and contact; we use Abaqus/Explicit (Simulia, Dassault Systemes, Providence, RI, USA) as finite element solver; the deforming vessel surface described above is meshed with 931 three-dimensional, 4-node surface elements with reduced integration (SFM3D4R).

Figure 4

2.2.2. Stent model

The analysis includes the idealized vessel model, previously described, and the stent model. In particular, we generate a model resembling the design feature of PRECISE Stent (Cordis Endovascular, a Johnson & Johnson company, Miami, FL), an open-cell self-expanding Nitinol stent commonly used for peripheral stenting. The model is based on high resolution micro-CT scans of the real device [12]; obviously we have to adapt the stent size to match the length of the device exploited for SFA/popliteal stenting. Consequently, we generate a stent model having in its free-expanded configuration an outer diameter of 8 mm and a length of 80 mm. The model mesh consists of 421,872 C3D8R elements and 787,500 nodes. To reproduce the superelastic material response, we use the Abaqus user material subroutine [13] of the superelastic model originally proposed by Auricchio and Taylor [14, 15]. The adopted Nitinol constitutive parameters are those reported in [16] (see Table 3).

3. Results

In the following, we present the results of our analysis with a particular focus on the popliteal kinematics and its effect on the stent solicitation estimated by structural FEA.

3.1. Popliteal kinematics

Given the vessel centerline, it is possible to compute several features of such a 3D curve, like length, curvature, and torsion. In our case, this data can be used to assess how the vessel shape changes during the leg bending. For this reason, we have computed the centerline of the popliteal artery in the straight and in the bent configuration, as mentioned in section 2.1, deriving the centerline features described in [17], as discussed in the following.

Shortening. The total length of the centerline is 224.58 mm for the straight case and 216.6 mm for the bent case, resulting thus in a light shortening, i.e., almost 5 %.

Curvature. The significant impact of the leg bending on the arterial shape is confirmed by the analysis of the centerline curvature resumed in table 1. In fact, the mean curvature of centerline obtained for the straight configuration is 0.0334 ($\pm$0.0209) mm^{-1}, while for the bent configuration is doubled, i.e., 0.0621($\pm$0.0387) mm^{-1}. Nevertheless, also the position of the point of maximum curvature changes, as

depicted in Figure 5: in the straight case, it is located at the middle of the vessel above the knee, while, after bending, it moves significantly upward (shift of 39.56 mm). In particular, the point of maximum point of curvature for the bent configuration clearly corresponds to the region where the vessel accommodates with a complex bending the knee flexion. The increase of the mean centerline curvature results also in a dramatic increase of the overall vessel tortuosity[1], i.e., +177%.

3.2. Stenting simulation

The results of the structural FEA are depicted in Figure 5, reporting different views of the deformed shape of the stent over-imposed to the lumen profile for both arterial configurations. From a qualitative point of view, it is possible to notice that the stent deployed in the artery when the leg is straight experiences a slight kink at the level of the proximal aneurysm neck (see posterior view in Figure 5); such a kink increases dramatically when the leg is bent, inducing a significant bending of the stent in this part of the vessel. These considerations clearly indicate that the stent experiences a non-uniform solicitation along its length, as further confirmed by a quantitative analysis of the computed stress reported in Table 2 and Figure 6. In particular, we split the stent (composed by 40 rings) in three parts, i.e., proximal (15 rings), middle (10 rings), and distal (15 rings), resembling the position of the stent portion within the artery. For each portion, we consider the computed von Mises stress at each integration point; given the lower threshold of 10 MPa, we compute the 99 percentile (VMS99) with respect to the volume of the stent part under investigation (i.e., only 1% of the considered volume has stress above this value) to neglect peak values due to local stress concentration. The results indicate that when the leg is straight the VMS99 is almost the same in all the stent portions while, when the leg is bent, the proximal part of the stent experiences an higher level of solicitation due to severe bending of the vessel below the knee. Such a bending is also inducing stent malapposition producing an overlapping of the struts (see Figure 7); this issue increases the potential risk of local stent failure and tissue damage; in fact, it has been hypothesized that this overlapping may increase the stent axial rigidity and also cause metal-to-metal hinge points initiating the fracture process due to fretting corrosion [19, 20, 7, 21].

4. Discussion

In the present study, we combine the use of medical image analysis and structural finite element analysis to evaluate how the configuration change of the popliteal artery, due to the knee flexion, deforms an implanted self-expanding stent. At the best of our knowledge, such an approach has not been presented in the literature yet; in fact, our analysis accounts for two of the three fields of analysis required to model the biomechanics of popliteal stenting: 1) the assessment of the arterial kinematics; 2) the simulation of peripheral stenting; 3) fatigue behaviour of Nitinol stents. The scientific literature regarding each of these three fields of investigation is notable but an integration of them is still missing. In the following, we discuss our findings with respect to some of the principal studies regarding the first two fields, leaving out the discussion of fatigue behaviour of Nitinol stents [22] because it is out of the scope of the present study.

Arterial kinematics. In their pioneering study of 1995, Wensing et al. [23] evaluated the morphology of the femoral artery during flexion and extension of the knee by examining 22 healthy volunteers with MRA; their results showed that the femoral and popliteal arteries became tortuous during knee flexion in all volunteers and the degree of tortuosity was age-dependent, as also confirmed by the study of Cheng et al. in 2010 [24]. Moreover, Wensing and colleagues explained well also the mechanisms of arterial bending due to knee flexion, which can be clearly observed from the medical image analysis of our study. The artery in the lower limb is positioned behind the axis of movement and this results in an excess of length when the leg is in flexed position; nevertheless, this issue is further enhanced by the fact that

[1]The lumen tortuosity index is defined as: $T = L/L' - 1$, with L, the centerline length, and L', the distance between the extreme points of the vessel [18]

the artery keeps to bend smoothly favouring physiologic hemodynamics. Such a length surplus can be accommodated by two mechanisms: i) part of it will be absorbed by the natural longitudinal elasticity of the vessel; ii) extra length leads to arterial tortuosity in the adductor canal and popliteal fossa. The latter effect is clearly visible from our results, e.g., in Figure 5, where the 3D complex bending of the artery increases when the leg is flexed, especially above the knee, leading to a significant stent solicitation in that region.

In 2005, Smouse et al. [25] measured SFA shortening during hip and knee flexion in a cadaver model. They evaluated seven human cadavers, i.e., 14 limbs, imaged on an angiographic table with respect to different hip flexion and knee bending to simulate walking, sitting-to-standing movement, and stair climbing. Their results suggest that the vessel bending occurs primarily, but not exclusively, behind the knee as also highlighted by our study. Moreover, they repeated all the measurements also after the insertion of Nitinol stents into the SFA and popliteal arteries. The authors underlined how, in case of stent implant, there is the possibility of catastrophic failure of the stent placed behind the knee due to kinking effect induced by the maximum flexion (squatting position). These considerations are also confirmed somehow by our study which highlights how the stent struts overlap in the region of higher curvature, underlying the potential risk of failure of the device in that region.

The *ex-vivo* results of Smouse and colleagues were subsequently integrated by Cheng et al. in 2006 [26] who quantified in vivo deformations of the superficial femoral artery during maximum knee and hip flexion with the use of magnetic resonance (MR) angiography. They analyzed the leg vasculature of eight healthy adults in the supine and fetal positions, computing the deformations induced by the leg flexion with the analysis of SFA centerline and its branches. They concluded that the high intra-individual variability of the vascular and muscular anatomy makes SFA lengths and deformations from the supine position to the fetal one unpredictable a priori; however, the data show that, from the supine position to the fetal position, the SFA tended to shorten and twist substantially, underlying the need to account such a mechanisms for the stent design. in 2009, Choi et al. [27] applied a new methodological approach for quantifying in vivo 3D arterial deformation due to pulsatile and non-pulsatile forces to a number of illustrative examples, e.g., the abdominal aorta, common iliac artery, SFA, and coronary artery. In particular, their results showed the significance of each deformation metric, revealing significant longitudinal strain and axial twist in the SFA and pronounced changes in vessel curvature inferior region of the SFA. If we compare our findings with their results regarding the distal part of the SFA (near the knee), it is possible to notice that in our case the mean curvature of the vessel centerline for the straight position is higher, i.e., 0.0334 mm^{-1} versus 0.008 mm^{-1}, but the difference between the mean curvatures, straight versus bent, is similar, i.e., 0.03 mm^{-1} versus 0.031mm^{-1}.

In this context it is also worth mentioning the review performed by Jonker and colleagues [28], who concluded that: i) SFA deformations depend on both age and degree of atherosclerosis; ii) SFA deformations cannot be assumed to be similar in different people; iii) if extensive kinking occurs during functional angiography (used as planning tool), the patient should either be excluded from stent placement or receive a more *elastic* or shorter stent.

Klein et al. [29] used paired angiographic images of overlapping segments of the femoro-popliteal artery in straight-leg and crossed-leg positions from patients with peripheral arterial disease, to quantify the conformational change of the artery between the two positions. Their results suggests that the changes in length, curvature, and twist are more significant in the popliteal artery than in the femoral one. In particular, the authors report a shortening of almost 15% for the poplitea, which is significantly higher than our outcomes.

Diehm et al. [30] proposed a study to assess if FEA can be used to predict deformation of the femoropopliteal segment during knee flexion. In particular, they analyzed the magnetic resonance angiography images of 8 healthy volunteers, taking the images with the lower limb fully extended and with the knee bent at 40°. Although the approach proposed by Diehm provides a good overall agreement with images, it has a high computational cost, while our approach is more straightforward and less computationally expensive because we reconstruct the vessel kinematics *mapping* the centerline deformation to an ideal

rigid vessel surface. At the same time, we acknowledge that this modeling strategy neglects the vessel deformability which can certainly play a role if a more realistic stent/artery interaction would be investigated. Unfortunately, Diehm et al. [30] do not report the centerline analysis so a direct quantitative comparison of our findings with their results is not feasible but, from a more qualitative point of view, the shape of artery at the maximum knee flexion as depicted in all cases studied in that paper appears to be smoother than the one reported in the present work. A partial justification of this could be the young age of the subjects investigated therein; in fact, in our case the patient is 66 years old while the subjects recruited in the Diehm's study are significantly younger (28 years as average); in fact, we know from the study of Wensing [23] that the degree of tortuosity is age-dependent, i.e., the older is the subject the more tortuous is the vessel.

In 2011, Ganguly et al. [31] proposed a direct method to study femoral artery stent deformations in vivo. Using a C-arm computed tomography system, the authors acquired the data of 13 consenting volunteers with stents in femoral vessels, imaging in straight and bent positions to observe stent deformations. The results suggest that the stents with the greatest change in eccentricity and curvature were located behind the knee or in the pelvis.

One year later, Young et al. [32] computed the arterial length change by means of a graphics-based anatomic and kinematic model of the lower extremity. They estimated an axial shortening of 23% for the femoro-popliteal arterial region characterized by a strong correlation with the maximum knee flexion angle but, surprisingly, their calculations showed that age was not a factor for influencing shortening or elongation.

Even more recently, Ghriallais and Bruzzi [33] proposed an anatomically accurate, 3D finite element model capable of capturing the loading conditions and deformation characteristics of the femoro-popliteal artery during knee flexion. The model is based on CT scan data and knee flexion was simulated and deformation characteristics of length change (axial compression), curvature, radial compression and axial twist were quantified. The authors compared the results of the knee bending simulation with experimental results available in literature [29, 27, 24] and not directly with the CT scan of the bent leg, which would be the straightforward option as highlighted by our study.

Finally, MacTaggart and colleagues [34] exploiting cadaver models demonstrated that 3D arterial bending, torsion and compression in the flexed lower limb are highly localized and are substantially more severe than previously reported.

Simulation of peripheral stenting. Rebelo and colleagues in 2009 [35] performed simulations of peripheral stenting obtaining a realistic artery geometry from magnetic resonance imaging scans of a patient in the fetal and supine positions, and comparing deformation of the stent deployed into the two different artery configurations. They took into account the effect of blood flow within the artery by performing a fluid-structure interaction simulation. Despite the study accounts for the main issues of stenting modeling, the authors considered a small portion of the SFA far from the popliteal artery and consequently the configuration change of the artery appears to be fairly limited when compared to our case.

Harvey in 2011 [36] evaluated through FEA the fatigue performance of two stent geometries: a helical stent design, and a more traditional straight strut, with a multiple crown design. Two vessel models were used by Harvey: i) a constant diameter straight tube; ii) a segment of the SFA obtained from CTA dataset. The author imposed two types of loading to the stent model through the vessel model: i) pulsatile loading resembling the blood pressure; ii) axial shortening and bending of the vessel model. Although the study proves the utility of combining advanced nonlinear finite element simulations and fatigue predictions for the design of peripheral Nitinol stents, the imposed loading conditions are rather idealized; our study suggested instead the importance to impose realistic, patient-specific loading conditions derived by medical image analysis.

In 2012, Petrini and colleagues [37] presented an integrated numerical and experimental approach for foreseeing Nitinol stent fatigue fracture based on: i) tests performed on Nitinol specimens with purposely-designed geometry, obtained from the same tubes and with the same procedure used in the production of commercial peripheral stents, ii) validation of a numerical model for the prediction of fatigue stent

behavior through the comparison with simple experimental tests, iii) tridimensional finite element analyses where, using a probabilistic approach (response surface), a wide range of in-vivo conditions are reproduced. This study was further integrated by Meoli and colleagues [38], who used FEA coupled to fatigue analysis to investigate two in vitro set-ups proposed by the literature [39, 40] and to increase the understanding of fatigue behaviour of commercial Nitinol stents. Their results indicate that the two investigated testing conditions produce quite a different fatigue behaviour both in terms of constant-life diagram and strain distribution in the stents. In particular, the results highlight that oversizing influence the fatigue behaviour of the devices with an effect on both the mean and amplitude values of the strain induced in the stents. Also in these studies, the imposed loading conditions are rather idealized, leaving room for further developments embedding patient-specific loading conditions derived by medical image analysis as suggested by our study.
All the discussed studies show how, since 1995 up to now, the scientific interest for the SFA/popliteal biomechanics has been always high and it is still motivating further investigation exploiting new technologies.

5. Limitations

Despite we base our study on the analysis of medical images of a real clinical case, the generalization of our results is not straightforward for the reasons illustrated in the following.
We have investigated just one clinical case, characterized by a popliteal aneurysm; such a disease is often treated through by-pass or stent-graft such as Viabahn (WL Gore and Associates, USA), while we simulate the implant of a bare metal stent used to treat atherosclerotic lesions. Such a discrepancy is in our opinion acceptable because the primary aim of the present study is to propose a modeling approach able to combine patient-specific medical images and structural finite element analysis to investigate popliteal stenting biomechanics. We acknowledge that it is necessary to account for both multiple cases and realistic implant conditions to obtain clinically-relevant considerations.
Moreover, we performed the structural analysis of stent loading due to knee bending under the hypothesis that stent does not influence the arterial kinematics, which keeps the same after the implant. We acknowledge that the robusteness of such an hypothesis should be further elucidated by a systematic comparison of the pre-stenting and post-stenting arterial shape in both straight and bent position; the available literature about this issue is still controversial: Arena [41] stated that stenting the proximal and mid-SFA generally does not severely alter the natural bend distally in the popliteal artery, but on occasion, it does intensify the bend; Smouse et al. [25] underlined that the rigidity may be drastically increased but this effect depends on the type of stent.

6. Conclusions

In the present study, we combine medical image analysis and structural finite element analysis to evaluate the solicitation of popliteal stent under patient-specific arterial kinematics. Our results indicate that the vessel changes significantly during the knee flexion leading to a non-uniform increase of the vessel curvature, especially above the knee. The resulting stent loading reflects such a non-uniform change of the arterial configuration; in fact, the stent portion located above the knee experiences a more severe solicitation than the remaining part of stent. Despite limited to one specific case, the study highlights the importance of non-uniform, complex, and three dimensional biomechanical solicitations for design of popliteal stents, underlining the potential key-role of dedicated patient-specific FEA simulations. In particular, from a prospective view, although a huge literature regarding the modelling and analysis of popliteal kinematics and its impact on stenting is available, the comparison of stenting simulation and reality is still lacking as well as a systematic comparison of the *in-vivo* arterial kinematics before and after the implant.

7. Conflict of interest statement

The authors have no commercial, proprietary, or financial interest in any products or companies described in this paper.

8. Acknowledgments

This work is partially funded by: ERC Starting Grant through the Project ISOBIO: Isogeometric Methods for Biomechanics (No. 259229); Ministero dell'Istruzione, dell'Universit e della Ricerca through the Project no. 2010BFXRHS; iCardioCloud project by Cariplo Foundation (No. 2013-1779)) and Lumbardy Region (No. 42938382; No. 46554874).
The authors acknowledge MD Mauro Ferrari (clinical support), Eng. Stefania Marconi (medical image elaboration) and the support of Regione Lombardia and CINECA Consortium through the grant LISA 2013 (high-performance computing).

References

[1] L. B. Wright, W. J. Matchett, C. P. Cruz, C. A. James, W. C. Culp, J. F. Eidt, T. C. McCowan, Popliteal artery disease: Diagnosis and treatment, Radiographics 24 (2) (2004) 467–479. doi:10.1148/rg.242035117.

[2] L. Norgren, W. Hiatt, J. Dormandy, M. Nehler, K. Harris, F. Fowkes, Inter-society consensus for the management of peripheral arterial disease (tasc ii), Journal of Vascular Surgery 45 (1, Supplement) (2007) S5 – S67. doi:http://dx.doi.org/10.1016/j.jvs.2006.12.037.

[3] H. Ravn, A. Wanhainen, M. Bjrck, Surgical technique and long-term results after popliteal artery aneurysm repair: Results from 717 legs, Journal of Vascular Surgery 46 (2) (2007) 236 – 243. doi:http://dx.doi.org/10.1016/j.jvs.2007.04.018.

[4] C. S. Cina, Endovascular repair of popliteal aneurysms, Journal of Vascular Surgery 51 (4) (2010) 1056 – 1060. doi:http://dx.doi.org/10.1016/j.jvs.2009.09.008.

[5] Y. Huang, P. Gloviczki, Popliteal artery aneurysms: Rationale, technique, and results of endovascular treatment, Perspectives in Vascular Surgery and Endovascular Therapy 20 (2) (2008) 201–213. doi:10.1177/1531003508320846.

[6] Y. Huang, P. Gloviczki, A. A. Noel, T. M. Sullivan, M. Kalra, R. E. Gullerud, T. L. Hoskin, T. C. Bower, Early complications and long-term outcome after open surgical treatment of popliteal artery aneurysms: Is exclusion with saphenous vein bypass still the gold standard?, Journal of Vascular Surgery 45 (4) (2007) 706 – 715.e1. doi:http://dx.doi.org/10.1016/j.jvs.2006.12.011.

[7] I. F. Tielliu, C. J. Zeebregts, G. Vourliotakis, F. Bekkema, J. J. van den Dungen, T. R. Prins, E. L. Verhoeven, Stent fractures in the hemobahn/viabahn stent graft after endovascular popliteal aneurysm repair, Journal of Vascular Surgery 51 (6) (2010) 1413 – 1418. doi:http://dx.doi.org/10.1016/j.jvs.2009.12.071.
URL http://www.sciencedirect.com/science/article/pii/S0741521410000364

[8] P. Yushkevich, J. Piven, H. Hazlett, R. Smith, S. Ho, J. Gee, G. Gerig, User-guided 3D active contour segmentation of anatomical structures: significantly improved efficiency and reliability, NeuroImage 31 (2006) 1116–1128.

[9] F. Auricchio, M. Conti, S. Marconi, A. Reali, J. L. Tolenaar, S. Trimarchi, Patient-specific aortic endografting simulation: From diagnosis to prediction, Computers in Biology and Medicine 43 (4) (2013) 386–394. doi:10.1016/j.compbiomed.2013.01.006.
URL http://www.sciencedirect.com/science/article/pii/S0010482513000206

[10] F. Auricchio, M. Conti, M. De Beule, G. De Santis, B. Verhegghe, Carotid Artery Stenting Simulation: from patient-specific images to Finite Element Analysis, Medical Engineering & Physics 33 (2011) 281–289.

[11] M. Conti, F. Auricchio, M. De Beule, B. Verhegghe, Numerical simulation of Nitinol peripheral stents: from laser-cutting to deployment in a patient specific anatomy, Proceeding of ESOMAT 2009 (2009) 06008doi:10.1051/esomat.

[12] M. Conti, D. Van Loo, F. Auricchio, M. De Beule, G. De Santis, B. Verhegghe, S. Pirrelli, A. Odero, Impact of carotid stent cell design on vessel scaffolding: a case study comparing experimental investigation and numerical simulations, Journal of Endovascular Therapy 18 (2011) 397–406.

[13] N. Rebelo, N. Walker, H. Foadian, Simulation of implantable stents, Abaqus User's Conference 143 (2001) 421–434.

[14] F. Auricchio, R. Taylor, Shape-memory alloys: macromodeling and numerical simulations of the superelastic behavior, Computer Methods in Applied Mechanics and Engineering 146 (1997) 281–312.

[15] J. Lubliner, F. Auricchio, Generalized plasticity and shape memory alloy, Int. J. Solid Strc 33 (1996) 991–1003.

[16] C. Kleinstreuer, Z. Li, C. Basciano, S. Seelecke, M. Farber, Computational mechanics of Nitinol stent grafts, Journal of Biomechanics 41 (2008) 2370–2378.

[17] M. Piccinelli, A. Veneziani, D. Steinman, A. Remuzzi, L. Antiga, A framework for geometric analysis of vascular structures: Application to cerebral aneurysms, IEEE TRANSACTIONS ON MEDICAL IMAGING 28 (8) (2009) 1141–1155.

[18] J. Thomas, L. Antiga, S. Che, J. Milner, D. Hangan Steinman, J. Spence, B. Kutt, D. Steinman, Variation in the Carotid Bifurcation Geometry of Young Versus Older Adults: Implications for Geometric Risk of Atherosclerosis, Stroke 36 (2005) 2450–6.

[19] D. Allie, C. Hebert, C. Walker, Nitinol stent fractures in the SFA, Endovascular Today (2004) 22–34.

[20] D. Scheinert, S. Scheinert, J. Sax, C. Piorkowski, S. Brunlich, M. Ulrich, G. Biamino, A. Schmidt, Prevalence and clinical impact of stent fractures after femoropopliteal stenting, Journal of the American College of Cardiology 45 (2) (2005) 312 – 315. doi:http://dx.doi.org/10.1016/j.jacc.2004.11.026.
URL http://www.sciencedirect.com/science/article/pii/S0735109704022570

[21] K. K. Kapnisis, D. O. Halwani, B. C. BrottPeter, G. Anderson, J. E. Lemons, A. S. Anayiotos, Stent overlapping and geometric curvature influence the structural integrity and surface characteristics of coronary nitinol stents, Journal of the Mechanical Behavior of Biomedical Materials 20 (2012) 227–236. doi:10.1016/j.jmbbm.2012.11.006.

[22] S. Robertson, A. Pelton, R. Ritchie, Mechanical fatigue and fracture of nitinol, International Materials Reviews 57 (1) (2012) 1–37.

[23] P. Wensing, F. Scholten, P. Buijs, M. Hartkamp, W. Mali, B. Hillen, Arterial tortuosity in the femoropopliteal region during knee flexion: a magnetic resonance angiographic study, Journal of Anatomy 187 (1) (1995) 133–139.

[24] C. Cheng, G. Choi, R. Herfkens, C. Taylor, The effect of aging on deformations of the superficial femoral artery resulting from hip and knee flexion: Potential clinical implications, Journal of vascular and interventional radiology 21 (2) (2010) 195–202.

[25] H. Smouse, A. Nikanorov, D. LaFlash, Biomechanical Forces in the Femoropopliteal Arterial Segment What happens during extremity movement and what is the effect on stenting?, Endovascular Today (2005) 60–66.

[26] C. P. Cheng, N. M. Wilson, R. L. Hallett, R. J. Herfkens, C. A. Taylor, In vivo {MR} angiographic quantification of axial and twisting deformations of the superficial femoral artery resulting from maximum hip and knee flexion, Journal of Vascular and Interventional Radiology 17 (6) (2006) 979 – 987. doi:http://dx.doi.org/10.1097/01.RVI.0000220367.62137.E8.

[27] G. Choi, C. Cheng, N. Wilson, C. Taylor, Methods for quantifying three-dimensional deformation of arteries due to pulsatile and nonpulsatile forces: Implications for the design of stents and stent grafts, Annals of Biomedical Engineering 37 (1) (2009) 14–33. doi:10.1007/s10439-008-9590-0.
URL http://dx.doi.org/10.1007/s10439-008-9590-0

[28] F. Jonker, F. Schlosser, F. Moll, B. Muhs, Dynamic forces in the sfa and popliteal artery during knee flexion, Endovascular Today (2008) 53–58.

[29] A. J. Klein, S. James Chen, J. C. Messenger, A. R. Hansgen, M. E. Plomondon, J. D. Carroll, I. P. Casserly, Quantitative assessment of the conformational change in the femoropopliteal artery with leg movement, Catheterization and Cardiovascular Interventions 74 (5) (2009) 787–798. doi:10.1002/ccd.22124.

[30] N. Diehm, S. Sin, H. Hoppe, I. Baumgartner, P. Büchler, Computational biomechanics to simulate the femoropopliteal intersection during knee flexion: a preliminary study, Journal of Endovascular Therapy 18 (3) (2011) 388–396.

[31] A. Ganguly, J. Simons, A. Schneider, B. Keck, N. R. Bennett, R. J. Herfkens, S. M. Coogan, R. Fahrig, In-vivo imaging of femoral artery nitinol stents for deformation analysis, Journal of Vascular and Interventional Radiology 22 (2) (2011) 244 – 249. doi:http://dx.doi.org/10.1016/j.jvir.2010.10.019.

[32] M. Young, M. Streicher, R. Beck, A. van den Bogert, A. Tajaddini, B. Davis, Simulation of lower limb axial arterial length change during locomotion, Journal of Biomechanics 45 (8) (2012) 1485–1490.

[33] R. Ghriallais, M. Bruzzi, Effects of knee flexion on the femoropopliteal artery: A computational study, Medical Engineering & Physics 35 (11) (2013) 1620 – 1628. doi:http://dx.doi.org/10.1016/j.medengphy.2013.05.015.
URL http://www.sciencedirect.com/science/article/pii/S135045331300132X

[34] J. N. MacTaggart, N. Y. Phillips, C. S. Lomneth, I. I. Pipinos, R. Bowen, B. T. Baxter, J. Johanning, G. M. Longo, A. S. Desyatova, M. J. Moulton, et al., Three-dimensional bending, torsion and axial compression of the femoropopliteal artery during limb flexion, Journal of biomechanics 47 (10) (2014) 2249–2256.

[35] N. Rebelo, R. Fu, M. Lawrenchuk, Study of a Nitinol Stent Deployed into Anatomically Accurate Artery Geometry and Subjected to Realistic Service Loading, Journal of Materials Engineering and Performance doi: 10.1007/s11665-009-9375-0 (2009) 655–663.

[36] S. Harvey, Nitinol stent fatigue in a peripheral human artery subjected to pulsatile and articulation loading, Journal of Materials Engineering and Performance 20 (4-5) (2011) 697–705.

[37] L. PETRINI, W. WU, E. DORDONI, A. MEOLI, F. MIGLIAVACCA, G. PENNATI, Fatigue behavior characterization of nitinol for peripheral stents, Functional Materials Letters 05 (01) (2012) 1250012.

[38] A. Meoli, E. Dordoni, L. Petrini, F. Migliavacca, G. Dubini, G. Pennati, Computational modelling of in vitro set-ups for peripheral self-expanding nitinol stents: The importance of stentwall interaction in the assessment of the fatigue resistance, Cardiovascular Engineering and Technology (2013) 1–11.

[39] A. Nikanorov, H. Smouse, K. Osman, M. Bialas, S. Shrivastava, L. Schwartz, Fracture of self-expanding nitinol stents stressed in vitro under simulated intravascular conditions, Journal of vascular surgery 48 (2) (2008) 435–440.

[40] S. Muller-Hulsbeck, P. Schafer, N. Charalambous, H. Yagi, M. Heller, T. Jahnke, Comparison of second-generation stents for application in the superficial femoral artery: An in vitro evaluation focusing on stent design, Journal of Endovascular Therapy 17 (6) (2010) 767–776.

[41] F. J. Arena, Arterial kink and damage in normal segments of the superficial femoral and popliteal arteries abutting nitinol stents a common, Vascular Disease Management 2 (5) (2005) 160–164.

Table 1: Centerline analysis.

	Straight	Bent	Δ
Lenght [mm]	224.58	213.6	-4.89%
Curvature [mm^{-1}]	0.0334±0.0209	0.0621±0.0387	+86%
Max curvature	0.1245	0.1965	+58%
Tortuosity	0.065	0.18	+177%

Table 2: Computed von Mises stress (VMS99) [MPa] for each stent portion (proximal, middle, distal) in each artery configuration (straight, bent).

	Straight	Bent	Δ
Proximal	319.080	448.519	+41%
Middle	345.249	372.723	+8%
Distal	325.558	364.216	+12%

Table 3: Adopetd Nitinol material properties [16].

Label	Description	Value
E_A	Austenite Young's modulus	35877 MPa
ν_A	Austenite Poisson's ratio	0.33
E_M	Martensite Young's modulus	24462 MPa
ν_M	Martensite Poisson's ratio	0.33
ε^L	Transformation strain	0.0555
$(d\sigma/dT)_L$	Loading temperature derivative of stress	0 MPa/°C
σ_L^S	Loading start of transformation stress	489 MPa
σ_L^E	Loading end of transformation stress	572 MPa
T_0	Temperature	22 °C
$(d\sigma/dT)_U$	Unloading temperature derivative of stress	0 MPa/°C
σ_U^S	Unloading start of transformation stress	230 MPa
σ_U^E	Unloading end of transformation stress	147 MPa
ρ	Density	6.5 g/cm^3

9. Figures

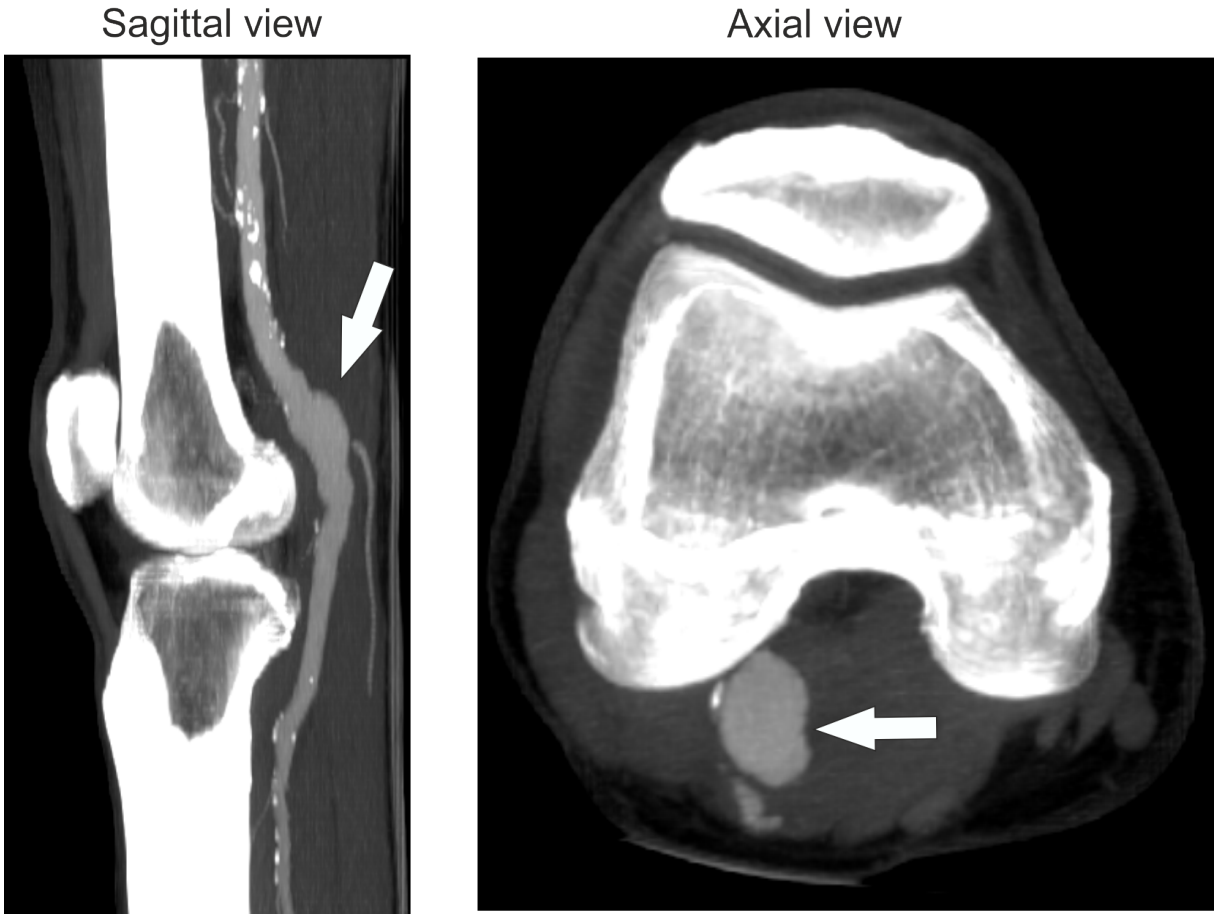

Figure 1: Sagittal and axial view of the popliteal aneurysm characterizing the clinical case under investigation. The white arrows indicate the location of the vascular lesion. The images are obtained using multiplanar reconstruction (MPR) tool of software Osirix [www.osirix.com]; the adopted thick slab is 29.06 mm.

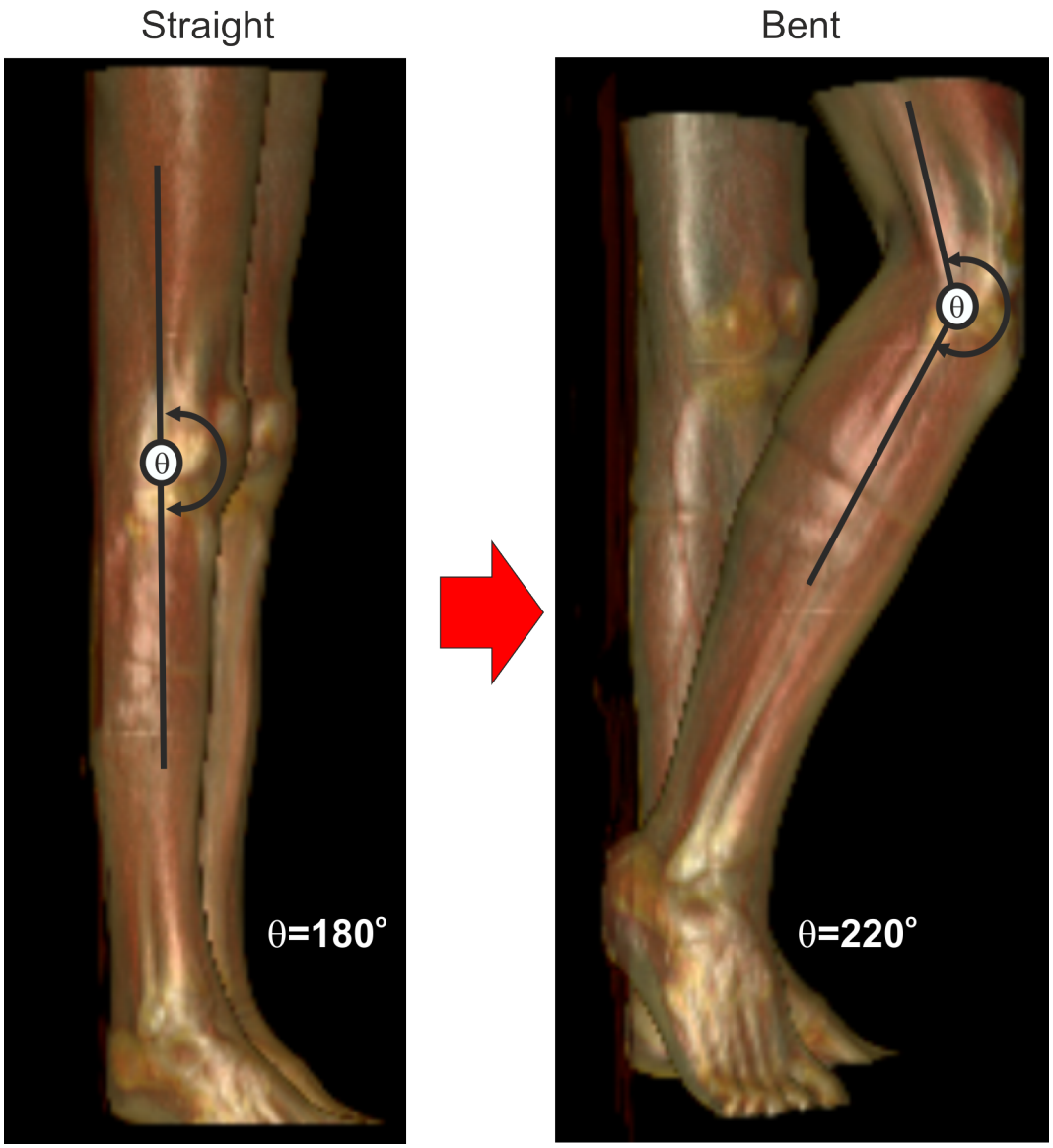

Figure 2: 3D volume rendering of the analyzed CTA datasets. The image highlights the right leg in straight (on the left) and bent (on the right) position. The considered angle θ between the upper and lower part of the leg is also depicted.

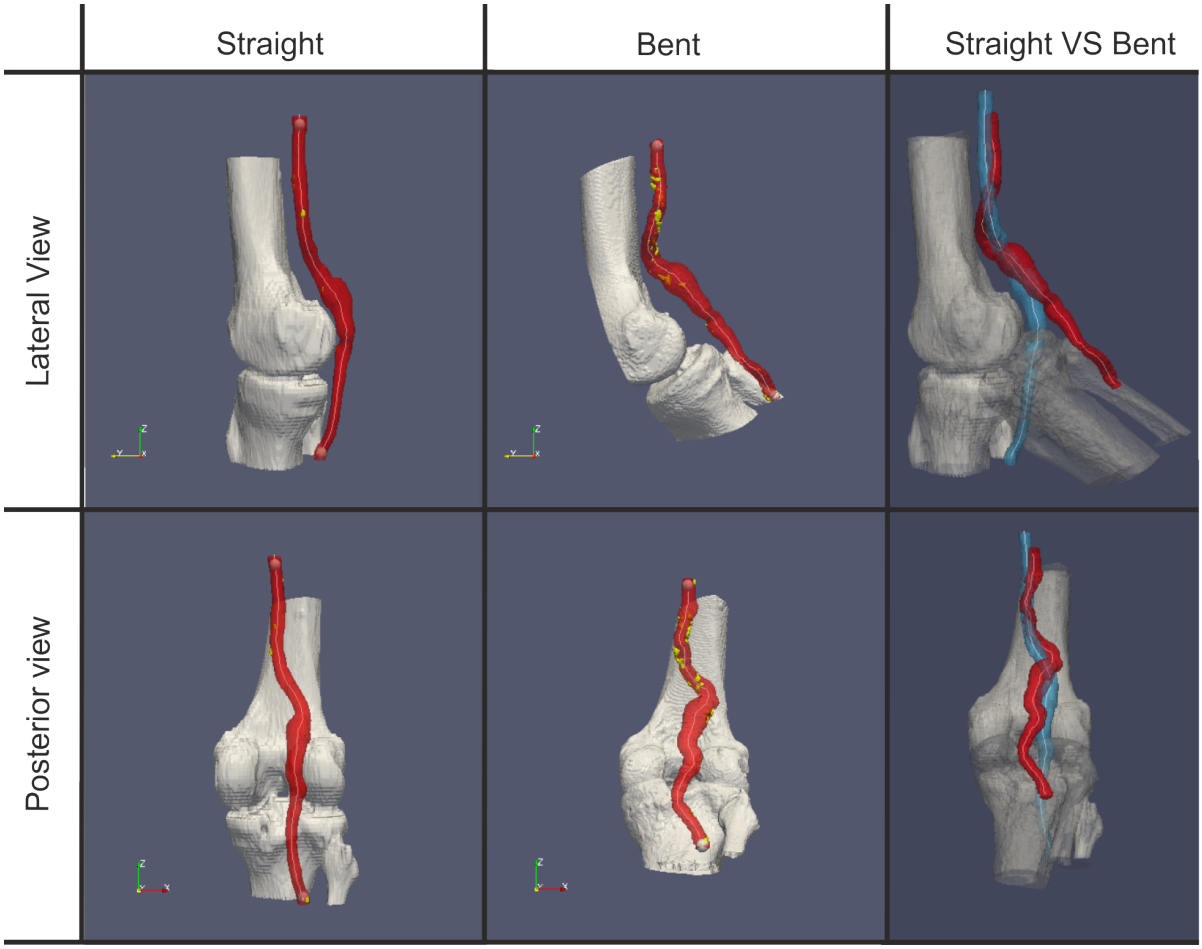

Figure 3: Different views of 3D reconstruction of the bone and popliteal artery for the straight configuration (left column) and bent configuration (right column). The right column of images depicts the superimposition of the two configurations to highlight the configuration change of the vessel. In the images also the lumen centerline and the vessel calcification are illustrated.

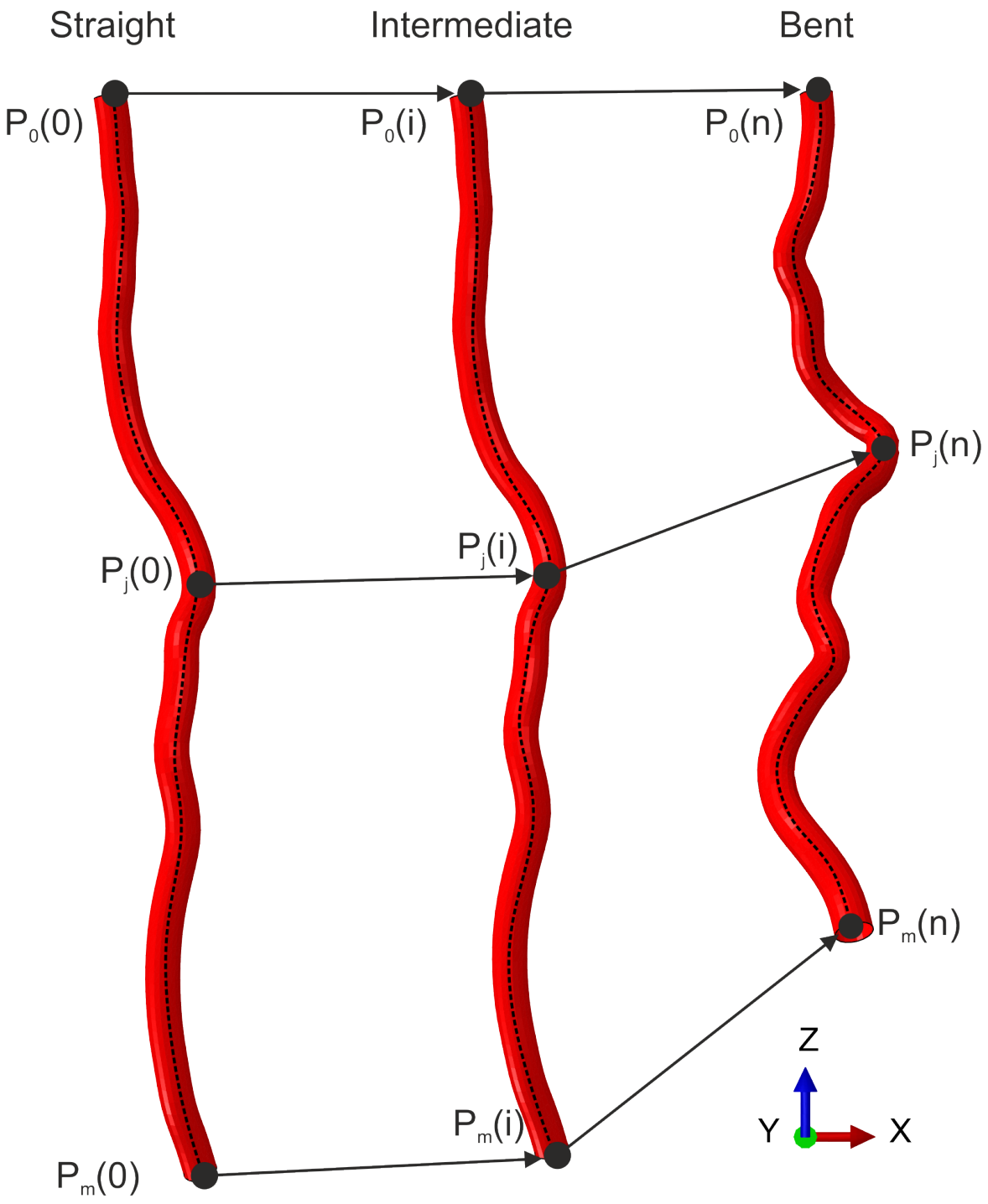

Figure 4: Schematic illustration of the arterial configuration change to be imposed as loading condition to the stent. The centerline is sampled with m equi-spaced points. Starting from the straight configuration (time T=0), the j-th point of the centerline $P_j(0)$ moves to the subsequent configuration (time T=i), $P_j(i)$, to finally reach the bent configuration at time T=n, $P_j(n)$.

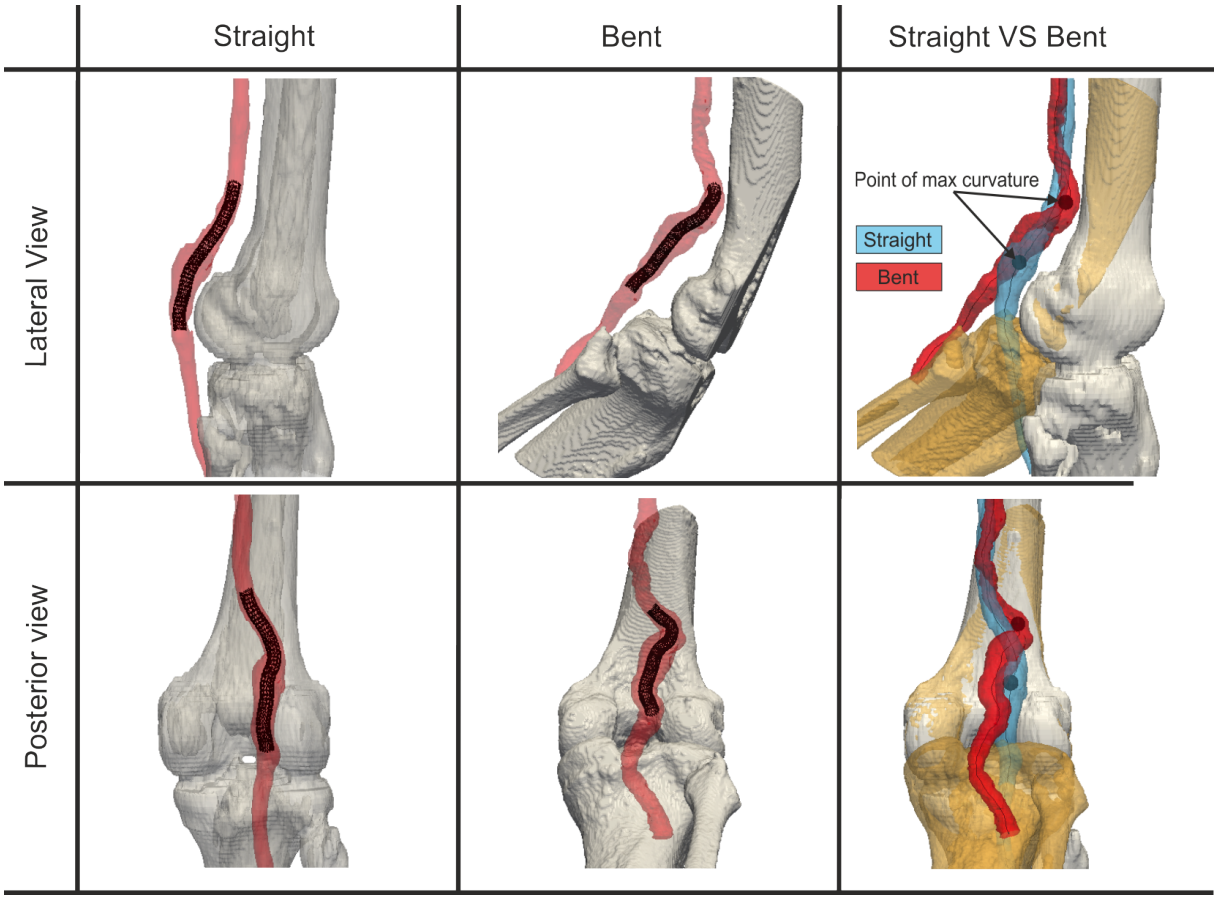

Figure 5: Stenting simulation and vessel centerline analysis: different views of the simulated results of stenting for the leg in straight position (left image column), after knee bending (middle image column) and position of the point of maximum curvature in both cases (right column). It is worth noting that the deforming surface imposing the kinematic change depicted in figure 4 is not illustrated here, this motivates the gap between the lumen profile and the stent which is deployed to a reference diameter of 6.8mm.

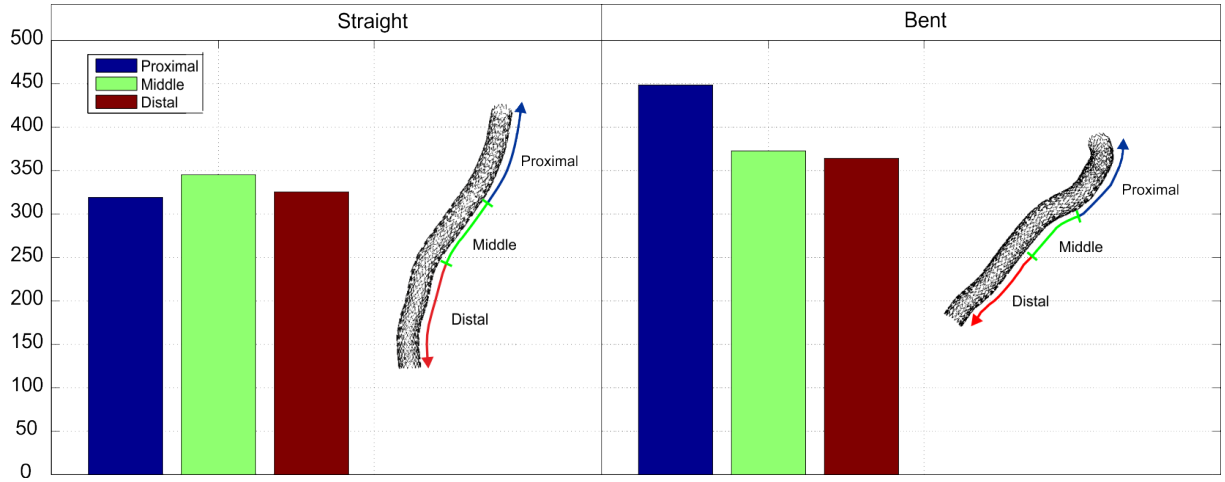

Figure 6: Bar plot of the von Mises stress (VMS99) [MPa] with respect three stent regions and the two configurations.

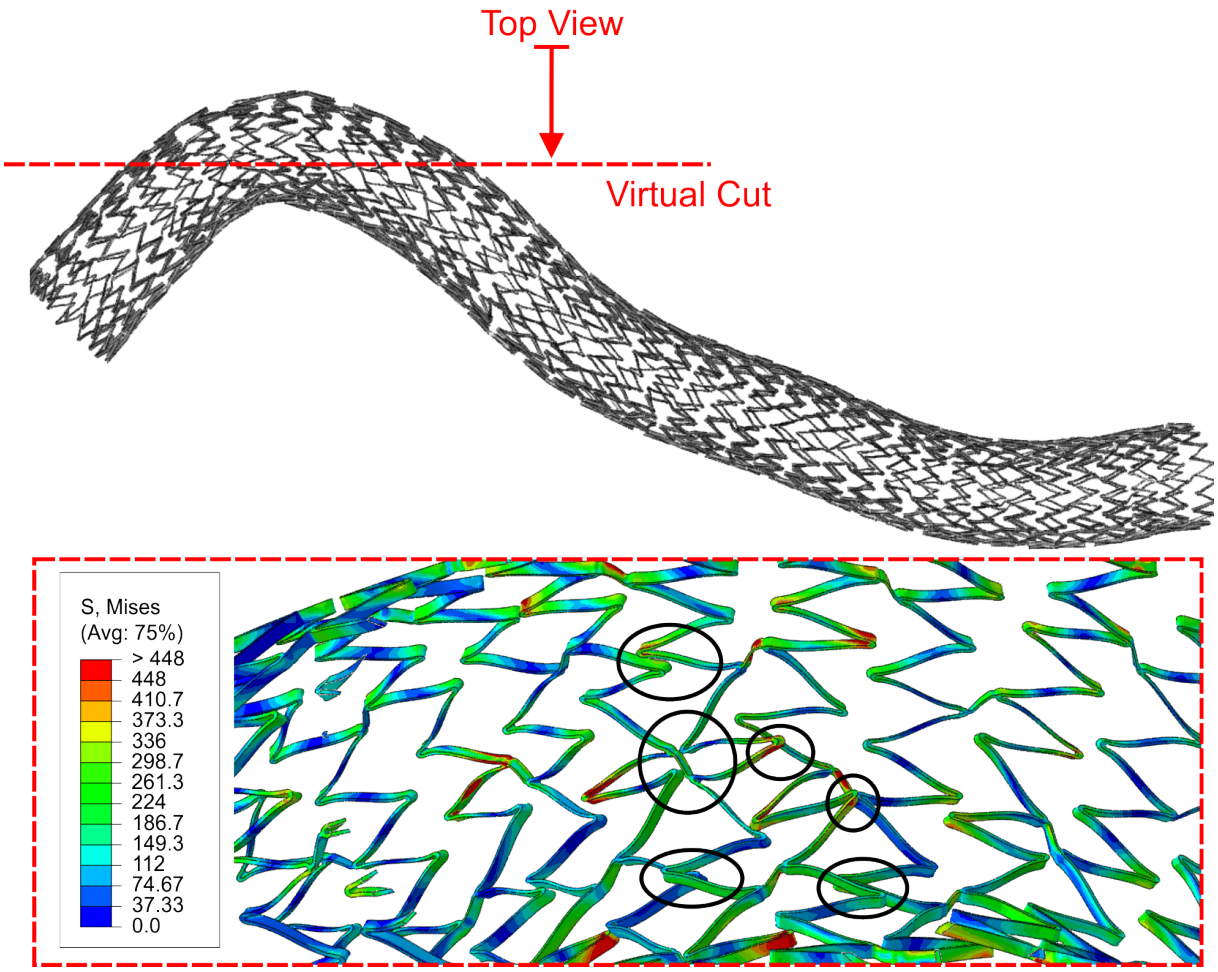

Figure 7: Stent configuration after the knee bending. The detail enclosed in the red box depicts the top view of a virtual cut of the stent structure, contoured by the computed von Mises stress [MPa]. The black circles over-imposed to the stent structure indicate the local strut overlapping induced by the vessel flexion in the region above the knee.